Use of solid-state NMR spectroscopy for investigating polysaccharide-based hydrogels

El Hariri El Nokab, Mustapha; Van Der Wel, Patrick C.a.

Published in:
Carbohydrate Polymers

DOI:
10.1016/j.carbpol.2020.116276

Publication date:
2020

Carbohydrate Polymers 240 (2020) 116276

Contents lists available at ScienceDirect

Carbohydrate Polymers

journal homepage: www.elsevier.com/locate/carbpol

Use of solid-state NMR spectroscopy for investigating polysaccharide-based hydrogels: A review

Mustapha El Hariri El Nokab, Patrick C.A. van der Wel*

Zernike Institute for Advanced Materials, University of Groningen, Nijenborgh 4, 9747 AG Groningen, the Netherlands

ARTICLE INFO

Keywords:
Solid-state NMR spectroscopy
^{13}C CP/MAS NMR
Alginate
Chitosan
Water-biopolymer interactions

ABSTRACT

Hydrogels find application in many areas of technology and research due to their ability to combine responsiveness and robustness. A detailed understanding of their molecular structure and dynamics (which ultimately underpin their functional properties) is needed for their design to be optimized and these hydrogels to be exploited effectively. In this review, we shed light on the unique capabilities of solid-state NMR spectroscopy to reveal this information in molecular detail. We review recent literature on the advancements in solid-state NMR techniques in resolving the structure, degree of grafting, molecular organization, water-biopolymer interactions and internal dynamical behavior of hydrogels. Among various solid-state NMR techniques, ^{13}C cross polarization (CP) magic angle spinning (MAS) NMR is examined for its ability to probe the hydrogel and its trapped solvent. Although widely applicable to many types of polymeric and supramolecular hydrogels, the current review focuses on polysaccharide-based hydrogels.

1. Introduction

Hydrogels are conventionally considered three-dimensional nanofibrous materials consisting of cross-linked hydrophilic polymer networks (Chai, Jiao, & Yu, 2017). They are able to swell and retain large amounts of water, while remaining insoluble and preserving their structural and dimensional constrained integrity due to the presence of chemical or physical cross links (Chivers & Smith, 2019). In addition to covalent cross-linking, the physical cross links can range from entanglements to weak formations of hydrogen bonds, Van der Waals interactions and π–π stacking. Hydrogels are often considered as biocompatible materials, since they possess high water content and a soft nature (Gun'ko, Savina, & Mikhalovsky, 2017). Moreover, in certain implementations they exhibit great similarity to natural extracellular matrices as well as cell adherence surfaces making them a suitable environment for cell proliferation (Dahlmann et al., 2013). Since their discovery and deployment in the biomedical field in the middle of the 20th century, hydrogels have been extensively studied and took a wide share in everyday products, but certain molecular aspects of their behavior and functionality remain incompletely understood (Yahia, 2015).

An interesting and useful subclass of hydrogels are stimuli-responsive hydrogels, also called smart hydrogels (Ebara et al., 2014; Ferreira et al., 2018; Samal, Dash, Dubruel, & Van Vlierberghe, 2014). These hydrogels undergo physicochemical transitions in response to external stimuli such as light, temperature, pressure, electric and magnetic fields as physical stimuli, or pH, ions and recognition events as chemical stimuli (Echeverria, Fernandes, Godinho, Borges, & Soares, 2018; Kopeček & Yang, 2012). Smart hydrogels based on physically cross-linked host-guest interactions, where noncovalent cross-linking points form the essential elements of the structure, are attracting particular attention nowadays (de Almeida et al., 2019; Tamesue, Takashima, Yamaguchi, Shinkai, & Harada, 2010; Yang & Zeng, 2013). Valuable properties and applications in drug delivery, tissue engineering, sensors, actuators, switching devices and several more biomedical applications are expected (Hamcerencu, Desbrieres, Popa, & Riess, 2012; Hamcerencu, Desbrieres, Popa, & Riess, 2009; Narayanaswamy & Torchilin, 2019; Vermonden, Censi, & Hennink, 2012; Yuk et al., 2019).

Much research is focused on designing particular gel-based biomaterials which mimic different functions of the extracellular matrices of body tissues (Caló & Khutoryanskiy, 2015; Guvendiren & Burdick, 2013; He et al., 2014). The network permeability, degree of grafting, drug release, and swelling behavior are critical parameters in evaluating the functional capability of hydrogels in their required applications (Amsden, Sukarto, Knight, & Shapka, 2007; Du et al., 2016; Ghorpade, Yadav, & Dias, 2016; Kono, Otaka, & Ozaki, 2014; Nardecchia et al., 2012; Singh & Singh, 2018; Singh, Dhiman, Rajneesh,

* Corresponding author.
E-mail addresses: m.el.hariri.el.nokab@rug.nl (M. El Hariri El Nokab), p.c.a.van.der.wel@rug.nl (P.C.A. van der Wel).

https://doi.org/10.1016/j.carbpol.2020.116276
Received 27 January 2020; Received in revised form 22 March 2020; Accepted 8 April 2020
Available online 21 April 2020

& Kumar, 2016; Singh, Varshney, Francis, & Rajneesh, 2016). These parameters are firmly linked to the structure and morphology of the gel network, in addition to the chemical nature of the composing polymer. It is these crucial parameters that are the main target for nuclear magnetic resonance (NMR) spectroscopy investigations (de Nooy, Capitani, Masci, & Crescenzi, 2000; Shapiro, 2011).

The most widely known use of NMR spectroscopy is in the liquid or solution state. In the solution state, small soluble molecules experience rapid thermal isotropic motions, which average out all orientation-dependent nuclear magnetic interactions. Then, isotropic components are the only detectable interactions left, resulting in highly resolved solution NMR spectra with excellent signal to noise. Problems arise for molecules that are in an immobilized or "solid" state, where they have restricted motions and are too big to tumble rapidly. This lack of sufficiently rapid isotropic mobility reveals in "solid-state" NMR studies the presence of different types of orientation-dependent nuclear and internuclear interactions (e.g. anisotropic and dipolar interactions) normally hidden in liquid-state NMR of small dissolved molecules. These interactions offer information on local geometric and electronic structure, but on the opposite side, are associated with the loss of resolution, reduced sensitivity and difficulties in the detection of individual atomic sites due to line broadening (Polenova, Gupta, & Goldbourt, 2015). In the absence of line-narrowing techniques (see below), the NMR spectra of most solids are broad and weak, limiting the insights accessible by this technique under such conditions.

Fortunately, several approaches have been developed to regain resolution and sensitivity. To suppress the anisotropic interactions dominating in solid-state, solid-state NMR is often combined with magic angle spinning (MAS). With this approach, the sample is rapidly rotated at an angle of 54.74° with respect to the static magnetic field of the NMR instrument. Undesired line-broadening interactions can be suppressed partially or totally depending on the MAS frequency, with total suppression occurring when the MAS frequency exceeds the magnitude of the interaction (Andrew, Bradbury, & Eades, 1959; Lowe, 1959). The result of this is a ssNMR spectrum with relatively narrow peaks occurring at the same isotropic chemical shift frequencies detected in liquid-state NMR spectroscopy. The use of ever faster MAS has dramatically enhanced the applicability and power of modern ssNMR.

Nowadays, solid-state NMR spectroscopy with its MAS-based techniques has established a firm position in the pharmaceutical and biomedical industry due to its ability to provide detailed molecular information in a nondestructive and noninvasive fashion. MAS NMR yields structural and molecular dynamical information, not only for crystalline structures, but also for amorphous and gel-like environments where other commonly used solid-state techniques have limited capabilities (Fu et al., 2011; Li et al., 2007; van der Wel, 2017, 2018; Weingarth & Baldus, 2013).

In Table 1 we summarize a few key differences in the use of solid- and liquid-state NMR, which will be further examined in the remainder of this review. Before examining recent applications to polysaccharide hydrogels, we discuss a few more general concerns and how to address them. One downside of spinning at ultra-high frequencies is the creation of frictional heating which can increase the sample temperature by up to 20 K and can be problematic if not compensated with active cooling, especially in case of thermo-responsive hydrogels (Aguilar-Parrilla, Wehrle, Bräunling, & Limbach, 1990; Brus, 2000; Dvinskikh, Castro, & Sandström, 2004; Langer, Schnell, Spiess, & Grimmer, 1999). MAS is often combined with a complementary line-narrowing technique based on the "decoupling" of line-broadening (dipolar) interactions with strong radio-frequency (RF) pulses. These decoupling sequences can also cause substantial sample heating, which is counteracted by additional sample cooling and improved probe designs (Gor'kov et al., 2007; Stringer et al., 2005). Another potential downside of the MAS approach is that it results in the MAS-rate-dependent generation of significant centrifugal forces that can damage sensitive samples (Han et al., 2010; Mandal, Boatz, Wheeler, & van der Wel, 2017; Renault, Shintu, Piotto, & Caldarelli, 2013). The safely achievable spinning frequency and the sample holder (known as MAS rotor) diameter are inversely proportional. Ultra-high spinning frequencies can only be reached with an accompanying reduction of the sample volume. Different types of MAS rotors are shown in Fig. 1 for size comparison. The displayed rotors have outer diameters of 7, 4, 3.2, 1.9 and 1.3 mm, corresponding to maximum internal sample volumes of approximately 240, 71, 30, 13 and 2.5 μL.

Whilst MAS dramatically improves the resolution and signal to noise of ssNMR, further signal enhancement techniques are important to overcome the inherently low sensitivity of the method. This is also connected to the small active volume of the employed MAS rotors (Fig. 1).^{13}C cross polarization (CP), which leverages the higher sensitivity and faster relaxation properties of ^{1}H nuclei, is one means to boost the signal of ^{13}C (and other less sensitive) nuclei. Moreover, it can be used to provide distinctive information not only on the molecular structure, but also on the molecular interactions, polymorphism, and chemical compositions of the hydrogel. This will be examined in more detail in the papers discussed in this review, which we focus primarily on illustrative recent alginate and chitosan hydrogels. Other noteworthy applications, of especially CP-based ssNMR, are also available on cellulose based materials (Courtenay et al., 2018; Isogai, Usuda, Kato, Uryu, & Atalla, 1989; Kono et al., 2002; Radloff, Boeffel, & Spiess, 1996; Schaefer & Stejskal, 1976; Sparrman et al., 2019). The high rigidity of especially crystalline cellulose makes CP ssNMR especially powerful, as it works optimally in rigid samples (Matlahov & van der Wel, 2018). It has been used to determine the cross-linking degree of superabsorbing networks, probing the network-additives interactions, identifying the solid state structural properties and packing arrangements, characterizing the polymorphic forms and conformational changes affecting the gelation properties (Capitani, Del Nobile, Mensitieri, Sannino, & Segre, 2000; Lenzi et al., 2003; Nonappa &

Table 1
Comparative table summarizing key differences between solid state and solution state NMR and in particularly the advantages of ^{13}C CP/MAS NMR for polysaccharide hydrogels.

	Solid-state NMR	Solution-state NMR
Sample type	All physical states are possible	Hydrolyzed gels only
Sample preparation	Simple and controllable preparation (hydration levels)	Time consuming preparation due to acid hydrolysis
Sample recovery	Yes	No
Challenges in hydrogels	Low resolution and sensitivity	Resolution depends on solubility
Detectable nuclei	^{1}H, ^{2}H, ^{13}C and several others	^{1}H mostly; more challenging for ^{13}C
Obtained information	Structure and dynamics of intact hydrogel	Chemical structure and composition

Fig. 1. Solid-state NMR sample sizes. Comparison (left to right) between the size of a 7 mm rotor spinning up to 7 kHz, a 4 mm rotor spinning up to 18 kHz, a 3.2 mm rotor spinning up to 24 kHz, a 1.9 mm rotor spinning up to 42 kHz and a 1.3 mm rotor spinning up to 70 kHz, including their driving caps, and that of a 2€ coin (far left).

Kolehmainen, 2016; Ramalhete et al., 2017). Nanochitosan and nanocellulose are of increasing interest in several fields including material science and biomedical engineering. ^{13}C CP/MAS NMR appears to be of significant importance in identifying the solid state structural properties and packing arrangements of these nanomaterials (Abitbol et al., 2016; Dufresne, 2019; Yang, Wang, Huang, & Hon, 2010).

The aim of this review is to examine the importance of solid-state NMR spectroscopy as a versatile analytical technique in resolving the structure *and* dynamics of a class of biomedical drug and cell delivery hydrogels. Hydrogels are classified as liquids, but behave like solids. The cross-linked nanofibrous network traps water, which in turn expands throughout its spacious volume, forming an insoluble non-fluid gel. These particular properties of a hydrogel make it suitable for use as a decent drug delivery system, allowing an encapsulation (and subsequent release) of target molecules in the trapped water phase. Hydrogels can be formed using different biological and chemical compounds including proteins, amyloid polypeptides, polysaccharides, organic and inorganic polymers (Butcher, Offeddu, & Oyen, 2014; Gibbs, Black, Dawson, & Oreffo, 2016; Naahidi et al., 2017). For biomedical applications bio-compatibility is an important consideration, leading to a particular interest in the development of polysaccharides as biocompatible drug delivery systems (Coviello, Matricardi, & Alhaique, 2006). Based on a combination of practical applications in biomedicine and the illustrative use of incisive ssNMR studies, we focus this review on recent CP MAS ssNMR studies of alginate and chitosan hydrogels.

2. Alginate

2.1. General properties

Alginate hydrogels show wide applicability as biocompatible materials; their porous structure along with their high water content enables the accommodation of high loads of water-soluble compounds. These properties made them state of the art for use as scaffolds in tissue engineering, vehicles for drug delivery and extracellular matrix models for biological studies (Lee & Mooney, 2012; Tønnesen & Karlsen, 2002).

Alginates are linear polysaccharides with a defined chemical structure assembled from a mixture of two types of monosaccharides (see Fig. 2 and below). Two different types of alginates are well known depending on the source of production: seaweed-derived and bacterial alginate. Seaweed-derived alginate is extracted with an aqueous alkali solution from brown algae (*Phaeophyceae*), including *Ascophyllum nodosum*, *Macrocystis pyrifera* and different *Laminaria* species. The addition of calcium chloride or other different cationic sources catalyzes the precipitation of the negatively charged alginate, to be followed by an acid treatment to form alginic acid. This production pathway is used in industry for the production of commercial products, due to its simplicity and low production cost (Smidsrød & Skjåk-Braek, 1990). The bacterial production pathway offers more options for tailored chemical structures and physical properties, but is considered more expensive. Bacterial alginate can be produced from *Pseudomonas aeruginosa* and

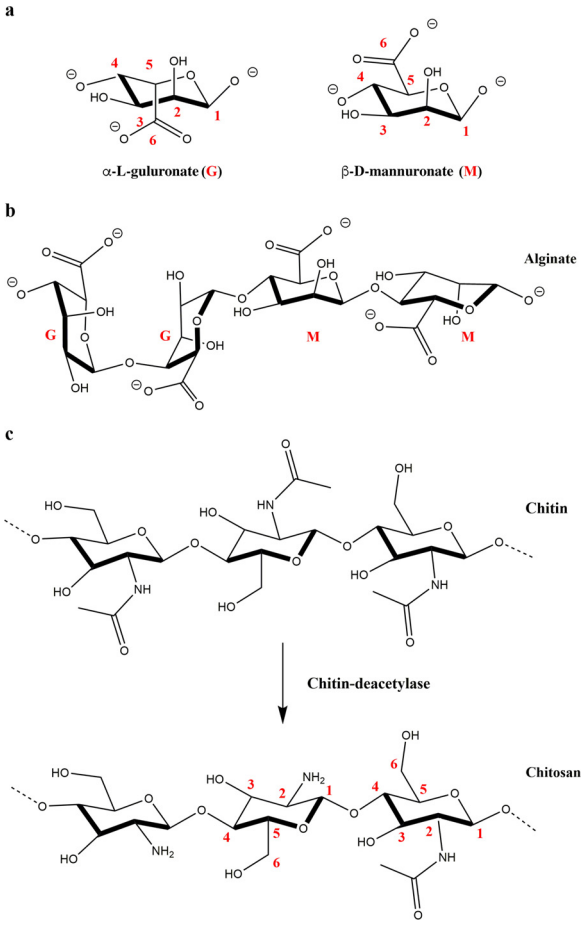

Fig. 2. Chemical structures of select mono- and polysaccharides. (a) Structures of D-mannuronate (M) and L-guluronate (G), with the numbering of carbon sites indicated. (b) Linear alginate chain consisting of D-mannuronic acid and L-guluronic acid units. (c) Chemical structures of chitin, as well as the linear chitosan (1,4)-linked D-glucosamine polymeric chain obtained after 66 % deacetylation starting from chitin. The numbering of the M and G carbon sites is also indicated.

Azotobacter vinelandii via similar procedures, although this approach yields alginate with G-blocks which form stronger gels with higher viscosity when cross-linked with Ca^{2+} ions (Remminghorst & Rehm, 2006; Silva et al., 2012; Urtuvia, Maturana, Acevedo, Peña, & Díaz-Barrera, 2017).

2.2. Structure and characterization

D-mannuronate (M) was thought to be the major component of alginate until the L-guluronate (G) subunit was also identified (Fig. 2) (Fischer & Dörfel, 1955). The chemical structure of alginate was distinguished later as series of block copolymers, consecutive G or M residues, and alternating M and G ones. Alginate composes a whole family of unbranched blocks of (1,4) linked β-D-mannuronate and α-L-guluronate residues. The M/G ratios are subjected to natural source variation, hence alginate extracted from different sources will differ in M and G content, length and sequence of the blocks (Gacesa, 1988; Thu et al., 1996). Several chromatographic and spectroscopic techniques were used for the structural analysis and M/G ratio determination of alginate hydrogels such as thin layer chromatography, ion-exchange chromatography, gas chromatography, solution-state NMR, IR, NIR and Raman spectroscopy (Salomonsen, Jensen, Stenbæk, & Engelsen, 2008; Usov, 1999).

Solution-state NMR is a common and extensively used technique,

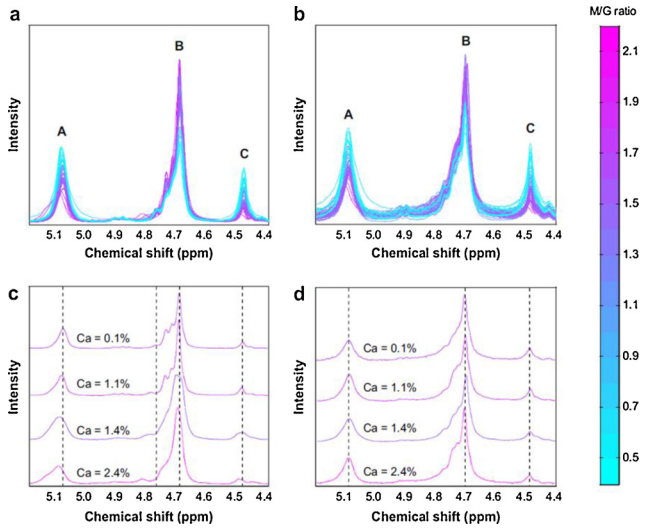

Fig. 3. Comparative solution- and solid-state NMR analysis. (a) H solution-state NMR spectra of hydrolyzed sodium alginate samples with variable M/G ratios, (b) ^{1}H MAS NMR spectra of intact sodium alginate samples soaked in D_2O, (c) four alginate samples cross linked with different calcium contents obtained by solution-state, and (d) by ^{1}H MAS NMR. Adapted with permission from reference (Salomonsen et al., 2009a).

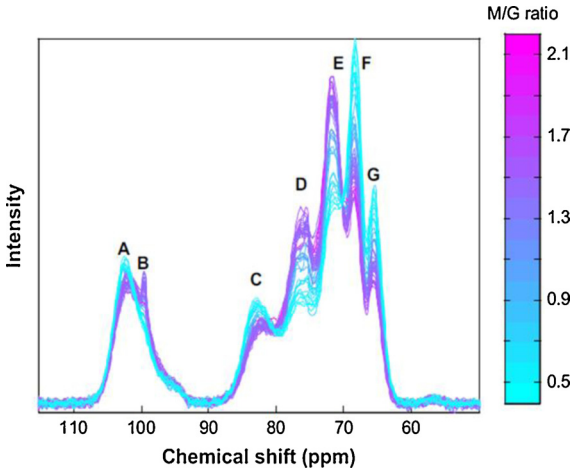

Fig. 4. Analysis of carbohydrate polymer content by solid-state NMR. Overlaid ^{13}C CP/MAS NMR spectra of 42 sodium alginate powders with different M/G ratios. Adapted with permission form (Salomonsen et al., 2009a).

but acid hydrolysis of the long polysaccharides is often essential for obtaining well-resolved spectra. Partial acid hydrolysis is considered time consuming and is sample destructive. Additionally, broad overlapping lines appear whenever suspended aggregates are present (Grasdalen, 1983). As noted above, in such liquid-state NMR spectra of large slowly tumbling molecules, a combination of chemical shift anisotropy and dipolar interactions, as caused by the reduced mobility of suspended aggregates, are the main causes of broadening. MAS NMR experiments can be used to suppress or overcome the broadening effects associated with these aggregated states. A comparison is shown in Fig. 3a-b between measurements done by ^{1}H solution-state NMR on hydrolyzed alginate and ^{1}H MAS NMR on *intact* alginate samples having various M/G ratios. The resolution and M/G ratios obtained by both techniques are comparable and in good agreement, without the need for hydrolysis for MAS NMR. Upon addition of calcium to the alginate, the negatively charged polysaccharide tends to cross-link into a hydrogel with reduced mobility. As shown in Fig. 3(c–d), upon increasing the calcium content, due to increase in sample viscosity, one observes line broadening and shifting of proton signals in ^{1}H solution-state NMR spectra. Under such conditions, ^{1}H MAS NMR is a powerful and alternative technique as the MAS helps suppress these line broadening effects. Thus, MAS NMR on crosslinked hydrogels can be useful to resolve the structure and determine the M/G ratios, especially as it bypasses the need for destructive and time-consuming acid hydrolysis procedures (Salomonsen, Jensen, Larsen, Steuernagel, & Engelsen, 2009a).

^{13}C CP/MAS NMR spectroscopy represents an additional technique that provides insight at the atomic-resolution level into alginate hydrogel structure and dynamics. Unlike the ^{1}H NMR mentioned above, here one detects the signal of ^{13}C isotopes present in the hydrogels (often at natural abundance). It is important to note that the peak intensities in ^{13}C CP/MAS NMR spectra are not usually quantitative measures. The reason for this is that the efficiency of CP-based magnetization transfer from ^{1}H to ^{13}C depends on the strength of the dipolar interaction between ^{1}H and ^{13}C, which varies across the molecule and depends on local mobility (Matlahov & van der Wel, 2018). That said, various techniques have been developed that much improve the reliability of quantitative interpretation of CP/MAS NMR (Hou et al., 2006; Johnson & Schmidt-Rohr, 2014; Takeda et al., 2012). Moreover, relative changes in peak intensity can be used to obtain valuable (semi) quantitative insights into the composition of different samples with similar characteristics.

The ^{13}C CP/MAS NMR spectra in Fig. 4 show the anomeric carbons around 101 ppm and the ring carbons in the range of 60 − 90 ppm (Mollica, Ziarelli, Lack, Brunel, & Viel, 2012; Salomonsen, Jensen, Larsen, Steuernagel, & Engelsen, 2009b; Sperger, Fu, Block, & Munson, 2011). Assignments of the alginate peaks from ^{13}C CP/MAS NMR (Salomonsen et al., 2009a) are shown in Table 2. Since solution and solid-state MAS NMR chemical shifts are directly comparable, assignments of the observed NMR signals are often performed with the support from ^{13}C solution-state NMR data. Similarly, M/G ratios are calculated and structural changes can be directly detected. However, the perturbation in the chemical shifts of neighboring residues often cannot be identified in the ^{13}C CP/MAS NMR spectra due to limited resolution.

It is worth noting that solid-state NMR generally suffers from a reduced resolution relative to typical high-resolution solution NMR data. This can stem from various sources, including the presence of structural heterogeneity, specific time scales and modes of dynamics, and limiting hardware specifications (including field strength and MAS rate). One of the key advances in modern solid-state NMR stems from an increased awareness of the controllable parameters that can improve the resolution. One key finding that is quite appreciable in biomolecular solid-state NMR (Mandal et al., 2017; Marassi & Crowell, 2003; Martin & Zilm, 2003), is that presence of optimized levels of hydration can be highly beneficial. Hydrated samples display increased mobility, which can both help and hurt the spectral resolution, depending on the timescale of motion. The dynamics (and thus resolution) may be tuned to some degree by modulating the solvent coupled dynamics based on changes in viscosity and sample temperature, among others (Li et al., 2019; Mandal et al., 2015; Sarkar et al., 2016). Complementing these sample optimization approaches, modern solid-state NMR can also offer improved resolution by increased access to high-field NMR instrumentation, ultrafast MAS equipment and new pulse sequence developments, facilitated in part by access to national and international shared facilities.

Table 2
Assignments of the ^{13}C CP/MAS NMR peaks of D-mannuronic acid and L-guluronic acid in Fig. 4. (Salomonsen et al., 2009a).

	Resonance						
	A	B	C	D	E	F	G
Chemical shift (ppm)	102.2	99.5	82.8	76.4	71.6	68.4	65.5
Assignments	G1	M1	G4	M4/M5	M3/M2	G3/G5	G2

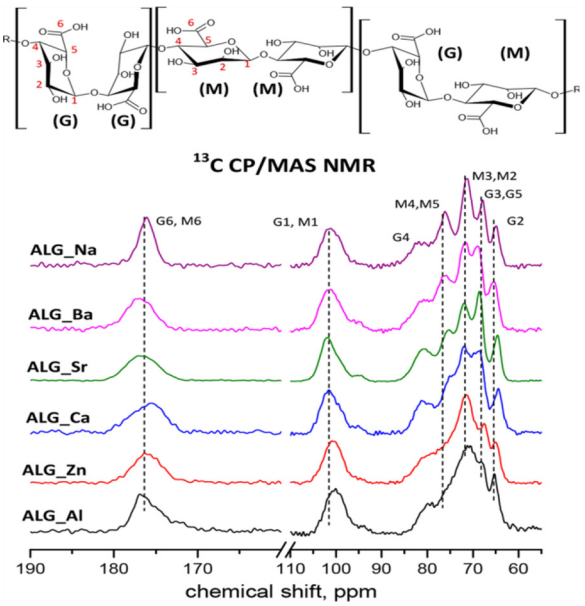

Fig. 5. Solid-state NMR detects cross-linker dependent structural changes. ^{13}C CP/MAS NMR stack plot for 6 alginate samples cross linked with different polyvalent cations. The spectra are arranged according to the ionic radii, from the largest (Ba^{2+}) ion to the smallest (Al^{3+}) ion. Adapted with permission from (Brus et al., 2017).

^{13}C CP/MAS NMR shows a clear difference in the local environment of the hydrogels formed by cross linking with different polyvalent cations (stack plot in Fig. 5). Broadening affects specific signals such as signals of carbonyl units ranging from 170 to 180 ppm and M unit pyranose rings around 75 ppm, undoubtedly indicating a distinct divergence in the local structures of the alginate hydrogels. A systematic relation was also observed between the increase in broadening of M signals and the decrease in the polyvalent ion size (Brus et al., 2017; Urbanova et al., 2019). The broadening and disappearance of the M4 and M5 carbon signals, while G units are substantially unaffected, point to a degree of conformational diversity of the MG, MM, and GG blocks, their interaction with the polyvalent cations and their role in forming stable complexes (Agulhon, Robitzer, David, & Quignard, 2012; Hecht & Srebnik, 2016).

Disregarding the different cationic species used for gel cross linking, the relatively narrow ^{13}C CP/MAS NMR signals reflect the uniformity of G-rich blocks in the measured hydrogels. The GM and MM blocks are expected to have a more open geometry than GG ones, thus further depending on the size, valence and affinity of interacting cationic species. Therefore, accepting more interchain aggregation and conformational flexibility. Alginate polymer chains are known to be rigid, but a certain degree of internal motion exists in strongly hydrated domains. The broadening observed in the ^{13}C CP/MAS NMR signals in Fig. 5 could be associated with the presence of segmental dynamics (Brus et al., 2017; Urbanova et al., 2019). Further solid-state NMR studies of these structural and motional aspects of these polysaccharide hydrogels are needed for a specific analysis and interpretation of these molecular features. Fortunately, solid-state NMR offers an array of complementary approaches that probe the local and overall dynamics of the system (Matlahov & van der Wel, 2018).

2.3. Local environment diversity

MAS NMR can also provide a direct view of the cross-links themselves. To investigate deeply the local environment near Al^{3+} ions in alginate gels, 2D ^{27}Al triple quantum (TQ) MAS NMR experiments have been used (Brus et al., 2017; Urbanova et al., 2019). Two distinct Al^{3+} sites appeared clearly at 0.3 and 1.4 ppm shown in Fig. 6. Moreover, the

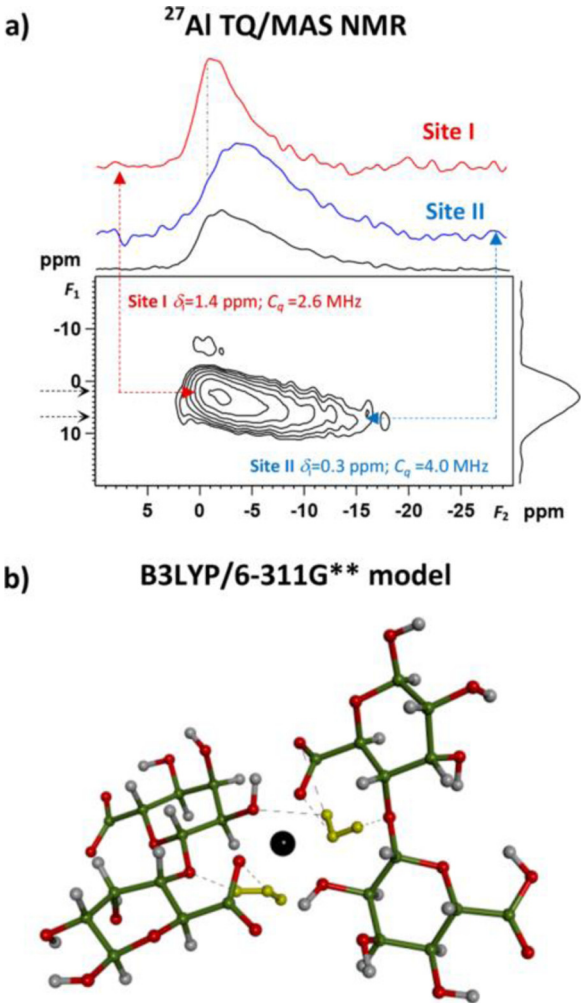

Fig. 6. Solid-state NMR analysis of hydrogel cross-linkers. (a) 2D ^{27}Al TQ/MAS NMR spectrum of an alginate sample cross-linked by Al^{3+}. The top shows the full 1D projection (black) and 1D slices extracted from the two observed Al^{3+} sites (red, blue). Adapted with permission from (Brus et al., 2017) (For interpretation of the references to colour in this figure legend, the reader is referred to the web version of this article.).

2D NMR analysis revealed that the octahedral coordination structure of Al^{3+} ions in the two sites showed distinct quadrupole coupling constants (C_q) of 4.0 and 2.6 MHz, respectively. That difference revealed the local coordination geometry for the site with $C_q = 2.6$ MHz to have a spherical symmetry, while the other site has significant distortions in the local symmetry. The two types of cross linking centers have comparable population, determined from the signal intensities. The motion of the water molecules and mobility of the central ions were found to be significant factors affecting the local dynamics (Brus et al., 2017; Urbanova et al., 2019).

3. Chitosan

3.1. General properties

Chitosan is a linear polysaccharide produced commercially by chemical modification (deacetylation) of chitin. Chitin is a cellulose-like biopolymer that is mainly found in the exoskeleton of aquatic marine animals such as shrimps, crabs, and lobsters, and cell walls of fungi. NMR spectroscopy is the most reliable technique to determine the degree of deacetylation, which ranges between 60–100 % for commercially available material. Chitosan was proposed as a promising

candidate for therapeutic applications and wound healing because of its properties as a cholesterol trapping agent, antioxidant, antibacterial and its hypoglycemic activity in the prevention of chronic diseases. The versatility of chitosan promoted its usage in waste management, agriculture, water purification, cosmetics, dentistry, food packaging and drug delivery systems (Hamedi, Moradi, Hudson, & Tonelli, 2018; Shariatinia, 2018).

3.2. Structure and degree of grafting

^{13}C CP/MAS NMR methods have proved useful for probing the chemical and structural conversions of chitosan and related biomass-derived materials. The technique has been used to evaluate the ability of thermal treatments to change the normally amorphous nature of carboxymethyl chitosan (CMC). All structures resulting from thermal treatment in ^{13}C CP/MAS spectra showed broad signals indicative of a wide distribution of local structures (Capitani, De Angelis, Crescenzi, Masci, & Segre, 2001). Therefore, thermal treatment did not result in a transformation of the amorphous structure of chitosan into a long-range crystalline defined one. The dynamics of the system could also be monitored by ^{13}C CP/MAS dynamic experiments. The solid-state NMR measurements determined the dipolar coupling between directly bonded ^{1}H and ^{13}C sites, based on the optimal CP contact time (0.5 and 0.4 ms for untreated and treated CMC samples, respectively) where the maximum signal to noise occurs in the ^{13}C spectra. As this coupling parameter is sensitive to dynamic averaging (manifest in reduced order parameters), its measurement by CP/MAS NMR can be used to probe local mobility. All values obtained for CMC fall in the very rigid range of values, representing relatively high dipolar coupling order parameters, although with a slight increase in order for the thermally treated sample (Di Colo et al., 2006).

^{13}C direct excitation, sometimes known as direct polarization, MAS ^{13}C NMR spectra provide a complementary method of measuring ^{13}C signals by MAS NMR. Under the right conditions, these direct-excitation experiments permit a more quantitative analysis than is achievable by standard CP-based MAS NMR (Hou et al., 2006; Kono & Teshirogi, 2015). This is due to the fact that these experiments are not reliant on ^{1}H-^{13}C dipolar couplings to polarize the ^{13}C signal (see also above). Such data are shown in Fig. 7 for cyclodextrin-grafted carboxymethyl chitosan (CD-*g*-CMC) and CMC hydrogels (Kono & Teshirogi, 2015). In these CMC samples, cyclodextrin (CD) units are attached to a subset of the CMC monosaccharide building blocks in order to facilitate the absorption properties toward acetylsalicylic acid (Aspirin), thus obtaining a biodegradable material possessing controlled on-demand drug release ability. These MAS NMR data provide significant structural information including ^{13}C resonance assignments and degree of grafting for carboxymethyl cyclodextran (CMCD). Overlap of the ^{13}C resonance peaks between CMC and those of CMCD occurs due to the chemical similarity and thus similarity of many of the chemical shifts. However, two peaks of CMC in the region of 52 − 58 ppm and 20 − 24 ppm, assigned to the C2 and the acetamide CH_3 group, can be distinguished separately from the peaks of CMCD. Additionally, several peaks in the range of 170 − 182 ppm region can be distinguished. The resonance at 178 ppm was assigned to carboxylate carbonyl carbons, while the one at 172 ppm was for amide carbonyl carbons and acetamide groups. Thus, by monitoring the appearance of these characteristic signals, MAS NMR allows for the detection of the incremental degrees of CD grafting. The graft degree of CMCD is considered as the average number of grafted CMCD per one monomer unit of CMC. The structural parameters obtained for each sample revealed clearly that an increase in the feeding ratio of CMCD to CMCs during the CD-*g*-CMC preparation procedure is followed by an increase in the degree of CD grafting in the gel network (Kono & Teshirogi, 2015; Kono, Onishi, & Nakamura, 2013; Kono, 2014).

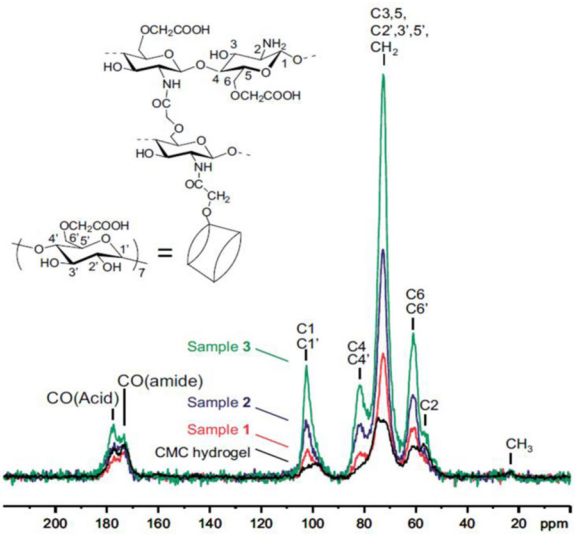

Fig. 7. Quantitative MAS NMR analysis of modified chitosan hydrogels. ^{13}C direct excitation MAS NMR spectra of CMC hydrogel and CD-g-CMC hydrogels. The spectra are normalized to the methyl carbon peak intensity at 22 ppm. ^{1}H-^{13}C dipolar decoupling was applied to enhance resolution. Adapted with permission from (Kono & Teshirogi, 2015).

3.3. Dynamic behavior of water molecules

Another valuable use of solid-state NMR is in the study of solvent interactions and solvent mobility within the hydrated hydrogels. The hydration characteristics of hydrogels are important for the mechanical and functional properties that are relevant for many applications. Variable temperature ^{2}H static NMR was previously used to determine the different water species in hydrated chitosan. Mobility of the water molecules is a major factor affecting the broadness of the ^{2}H NMR peaks such that: rigid components having restriction in mobility experience strong quadrupole interactions, thus leading to a broad peak. Meanwhile, mobile components having more freedom in mobility express weak quadrupole interactions, thus leading to a narrow peak. At room temperature, the broad peak of the rigid ^{2}H component is assigned to deuterons present as ND/OD, which experience rapid exchange with D_2O. The narrow peak of the mobile ^{2}H component is assigned to the weakly bound and free water, which experience higher mobility upon temperature increase. Upon decreasing the temperature to 190 K, the study observed coexistence of strongly bounded water to the biopolymer matrix, in a rigid amorphous form, non-freezable water exhibiting high mobility and flipping water that are immobilized and are able to undergo a 180° flip similar to crystalline hydrates. Therefore, four water species shown in Fig. 8 were identified: free water experiencing unrestricted motion, highly mobile but weakly bound

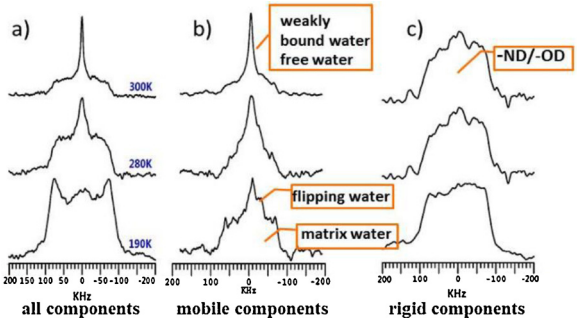

Fig. 8. Solid-state NMR analysis of water mobility within chitosan hydrogels. Variable temperature ^{2}H static NMR spectra of chitosan samples indicating the four different water species. Adapted with permission from (Wang, Zhang, Chen, & Sun, 2016).

water, rigid non-freezable matrix waters, and flipping water.

Although the solid-state NMR studies above are applied to polysaccharide samples in which the molecules are present randomly in all possible orientations (a powder distribution), solid-state NMR studies can also be applied to (partly) oriented or aligned samples. For example, compared to completely random orientations of deuterons present as ND/OD in a normal powder, alignment along the magic angle in static mode yields distinct NMR spectra. This method of preparing the sample has allowed insight into the structuring and orientation of the polymeric chain, for example in presence and absence of stretching forces. Thus information can be obtained via solid-state NMR that examines the important role of solvation water on the toughness, structure, and material properties of biomaterials (Radloff et al., 1996; Wang, Zhang, Chen, & Sun, 2016).

4. Conclusions and future perspectives

Various models and theories have been presented and enormous efforts have been made to understand the interpenetrating network, packing and mobility of hydrogels, but still limitations exist and controversies are not uncommon. Our understanding of the structural and chemical aggregation transformations, and water-matrix interaction pathways occurring in hydrogels is still limited (Hoffman, 2012). Fundamental progress in this direction can pave the way for designing the next generation of polysaccharide hydrogels. As we have seen, solid-state NMR spectroscopy is a promising technique in resolving as-yet missing aspects of the molecular structure, polymorphism, packing and dynamics of hydrogels. This is true for the systems examined above, as well as other nano-polysaccharides such as nanocellulose e.g. (nanofibrils and nanocrystals) and nanochitosan. These bio-derived materials may enable impressive and promising applications in different fields, which however require a deeper understanding of their molecular underpinnings. As we have tried to emphasize, one strength of modern solid-state NMR is its diversity of methods and ability to reveal many different aspects of molecular structure, dynamics and interactions. It is important to note that the work discussed above is just a modest, but hopefully informative, sampling of an ever growing literature.

There is substantial reason to be further optimistic about an even greater expansion of capabilities for the studying polysaccharide hydrogels. The reason for this is the ongoing advancements in solid-state NMR instrumentations and techniques, inspired by the world of biomolecular ssNMR and studies of non-hydrogel materials. Dramatic improvements in sensitivity can be gained by combining novel techniques such as ultrafast MAS (at rates exceeding 100 kHz) as well as dynamic nuclear polarization (DNP). Spectroscopic sensitivity is a critical parameter upon studying nanofibrous interpenetrating systems. DNP permits large signal enhancements overcoming sensitivity limitations, however also requires very low temperatures which could affect the behavior of the hydrogel (Kaplan et al., 2015; Koers et al., 2014; Mance et al., 2017; Medeiros-Silva et al., 2018; Smith et al., 2018). One exciting aspect of ultrafast MAS probeheads is that they can enable ^{1}H-detection with and without deuteration (Baker et al., 2018; Mance et al., 2015). An important factor in biomolecular ssNMR is the use of advanced isotopic labelling approaches (Baker & Baldus, 2014; Baker, Daniëls, van der Cruijsen, Folkers, & Baldus, 2015; van Zandvoort et al., 2015), which may also be valuable in future studies of polysaccharide hydrogels. An essential part of optimal use of solid-state NMR will be the pursuit of integrated methods, such as the combination of experimental solid-state NMR with ever-improving computational approaches (Rad-Malekshahi et al., 2015; Weingarth et al., 2012), and microscopic analysis such as Atom Probe Tomography and Cryo-Electron Tomography (Baker et al., 2018; Schmidt et al., 2018). Thus, based on the current literature, there is ample room for the increased application of the power and versatility of modern solid-state NMR to elucidate important features of responsive and non-responsive hydrogels. As illustrated by the work discussed in the current article, and the much broader solid-state NMR literature, great opportunities are available to learn about the structure, cross-linking, packing and mobility of interpenetrating gel networks formed by polysaccharides and other biopolymers alike.

Acknowledgments

This work was supported by financial support from the Zernike Institute for Advanced Materials at the University of Groningen, including funding from the Bonus Incentive Scheme (of the Dutch Ministry for Education, Culture and Science (OCW)).

References

Abitbol, T., Rivkin, A., Cao, Y., Nevo, Y., Abraham, E., Ben-Shalom, T., et al. (2016). Nanocellulose, a tiny fiber with huge applications. *Current Opinion in Biotechnology, 39*, 76–88. https://doi.org/10.1016/j.copbio.2016.01.002.

Aguilar-Parrilla, F., Wehrle, B., Bräunling, H., & Limbach, H.-H. (1990). Temperature gradients and sample heating in variable temperature high speed MAS NMR spectroscopy. *Journal of Magnetic Resonance, 87*(3), 592–597. https://doi.org/10.1016/0022-2364(90)90315-Z (1969).

Agulhon, P., Robitzer, M., David, L., & Quignard, F. (2012). Structural regime identification in ionotropic alginate gels: Influence of the cation nature and alginate structure. *Biomacromolecules, 13*(1), 215–220. https://doi.org/10.1021/bm201477g.

Amsden, B. G., Sukarto, A., Knight, D. K., & Shapka, S. N. (2007). Methacrylated glycol chitosan as a photopolymerizable biomaterial. *Biomacromolecules, 8*(12), 3758–3766. https://doi.org/10.1021/bm700691e.

Andrew, E. R., Bradbury, A., & Eades, R. G. (1959). Removal of dipolar broadening of nuclear magnetic resonance spectra of solids by specimen rotation. *Nature, 183*(4678), 1802. https://doi.org/10.1038/1831802a0.

Baker, L. A., & Baldus, M. (2014). Characterization of membrane protein function by solid-state NMR spectroscopy. *Current Opinion in Structural Biology, 27*, 48–55. https://doi.org/10.1016/j.sbi.2014.03.009.

Baker, L. A., Daniëls, M., van der Cruijsen, E. A. W., Folkers, G. E., & Baldus, M. (2015). Efficient cellular solid-state NMR of membrane proteins by targeted protein labeling. *Journal of Biomolecular NMR, 62*(2), 199–208. https://doi.org/10.1007/s10858-015-9936-5.

Baker, L. A., Sinnige, T., Schellenberger, P., de Keyzer, J., Siebert, C. A., Driessen, A. J. M., et al. (2018). Combined ^{1}H-detected solid-state NMR spectroscopy and electron cryotomography to study membrane proteins across resolutions in native environments. *Structure, 26*(1), https://doi.org/10.1016/j.str.2017.11.011 161-170.e3.

Brus, J. (2000). Heating of samples induced by fast magic-angle spinning. *Solid State Nuclear Magnetic Resonance, 16*(3), 151–160. https://doi.org/10.1016/S0926-2040(00)00061-8.

Brus, J., Urbanova, M., Czernek, J., Pavelkova, M., Kubova, K., Vyslouzil, J., et al. (2017). Structure and dynamics of alginate gels cross-linked by polyvalent ions probed via solid state NMR spectroscopy. *Biomacromolecules, 18*(8), 2478–2488. https://doi.org/10.1021/acs.biomac.7b00627.

Butcher, A. L., Offeddu, G. S., & Oyen, M. L. (2014). Nanofibrous hydrogel composites as mechanically robust tissue engineering scaffolds. *Trends in Biotechnology, 32*(11), 564–570. https://doi.org/10.1016/j.tibtech.2014.09.001.

Caló, E., & Khutoryanskiy, V. V. (2015). Biomedical applications of hydrogels: A review of patents and commercial products. *European Polymer Journal, 65*, 252–267. https://doi.org/10.1016/j.eurpolymj.2014.11.024.

Capitani, D., De Angelis, A. A., Crescenzi, V., Masci, G., & Segre, A. L. (2001). NMR study of a novel chitosan-based hydrogel. *Carbohydrate Polymers, 45*(3), 245–252. https://doi.org/10.1016/S0144-8617(00)00255-1.

Capitani, D., Del Nobile, M. A., Mensitieri, G., Sannino, A., & Segre, A. L. (2000). ^{13}C solid-state NMR determination of cross-linking degree in superabsorbing cellulose-based networks. *Macromolecules, 33*(2), 430–437. https://doi.org/10.1021/ma9914117.

Chai, Q., Jiao, Y., & Yu, X. (2017). Hydrogels for biomedical applications: Their characteristics and the mechanisms behind them. *Gels, 3*(1), 6. https://doi.org/10.3390/gels3010006.

Chivers, P. R. A., & Smith, D. K. (2019). Shaping and structuring supramolecular gels. *Nature Reviews Materials, 1*. https://doi.org/10.1038/s41578-019-0111-6.

Courtenay, J. C., Ramalhete, S. M., Skuze, W. J., Soni, R., Khimyak, Y. Z., Edler, K. J., et al. (2018). Unravelling cationic cellulose nanofibril hydrogel structure: NMR spectroscopy and small angle neutron scattering analyses. *Soft Matter, 14*(2), 255–263. https://doi.org/10.1039/C7SM02113E.

Coviello, T., Matricardi, P., & Alhaique, F. (2006). Drug delivery strategies using polysaccharidic gels. *Expert Opinion on Drug Delivery, 3*(3), 395–404. https://doi.org/10.1517/17425247.3.3.395.

Dahlmann, J., Krause, A., Möller, L., Kensah, G., Möwes, M., Diekmann, A., et al. (2013). Fully defined in situ cross-linkable alginate and hyaluronic acid hydrogels for myocardial tissue engineering. *Biomaterials, 34*(4), 940–951. https://doi.org/10.1016/j.biomaterials.2012.10.008.

de Almeida, P., Jaspers, M., Vaessen, S., Tagit, O., Portale, G., Rowan, A. E., et al. (2019). Cytoskeletal stiffening in synthetic hydrogels. *Nature Communications, 10*(1), https://doi.org/10.1038/s41467-019-08569-4.

de Nooy, A. E. J., Capitani, D., Masci, G., & Crescenzi, V. (2000). Ionic polysaccharide hydrogels via the Passerini and Ugi multicomponent condensations: Synthesis, behavior and solid-state NMR characterization. *Biomacromolecules, 1*(2), 259–267. https://doi.org/10.1021/bm005517h.

Di Colo, G., Baggiani, A., Zambito, Y., Mollica, G., Geppi, M., & Serafini, M. F. (2006). A new hydrogel for the extended and complete prednisolone release in the GI tract. *International Journal of Pharmaceutics, 310*(1–2), 154–161. https://doi.org/10.1016/j.ijpharm.2005.12.002.

Du, J., Li, B., Li, C., Zhang, Y., Yu, G., Wang, H., et al. (2016). Tough and multi-responsive hydrogel based on the hemicellulose from the spent liquor of viscose process. *International Journal of Biological Macromolecules, 88*, 451–456. https://doi.org/10.1016/j.ijbiomac.2016.04.013.

Dufresne, A. (2019). Nanocellulose processing properties and potential applications. *Current Forestry Reports, 5*(2), 76–89. https://doi.org/10.1007/s40725-019-00088-1.

Dvinskikh, S. V., Castro, V., & Sandström, D. (2004). Heating caused by radiofrequency irradiation and sample rotation in ^{13}C magic angle spinning NMR studies of lipid membranes. *Magnetic Resonance in Chemistry, 42*(10), 875–881. https://doi.org/10.1002/mrc.1477.

Ebara, M., Kotsuchibashi, Y., Uto, K., Aoyagi, T., Kim, Y.-J., Narain, R., ... Hoffman, J. M. (2014). Smart hydrogels. In M. Ebara, Y. Kotsuchibashi, R. Narain, N. Idota, Y.-J. Kim, J. M. Hoffman, ... T. Aoyagi (Eds.). *Smart biomaterials* (pp. 9–65). Japan: Springer. https://doi.org/10.1007/978-4-431-54400-5_2.

Echeverria, C., Fernandes, S., Godinho, M., Borges, J., & Soares, P. (2018). Functional stimuli-responsive gels: Hydrogels and microgels. *Gels, 4*(2), 54. https://doi.org/10.3390/gels4020054.

Ferreira, N. N., Ferreira, L. M. B., Cardoso, V. M. O., Boni, F. I., Souza, A. L. R., & Gremião, M. P. D. (2018). Recent advances in smart hydrogels for biomedical applications: From self-assembly to functional approaches. *European Polymer Journal, 99*, 117–133. https://doi.org/10.1016/j.eurpolymj.2017.12.004.

Fischer, F. G., & Dörfel, H. (1955). Die Polyuronsäuren der Braunalgen (Kohlenhydrate der Algen I). *Hoppe-Seyler´s Zeitschrift für physiologische Chemie, 302*, 186–203. https://doi.org/10.1515/bchm2.1955.302.1-2.186 (Jahresband).

Fu, R., Wang, X., Li, C., Santiago-Miranda, A. N., Pielak, G. J., & Tian, F. (2011). In situ structural characterization of a recombinant protein in native Escherichia coli membranes with solid-state magic-angle-spinning NMR. *Journal of the American Chemical Society, 133*(32), 12370–12373. https://doi.org/10.1021/ja204062v.

Gacesa, P. (1988). Alginates. *Carbohydrate Polymers, 8*(3), 161–182. https://doi.org/10.1016/0144-8617(88)90001-X.

Ghorpade, V. S., Yadav, A. V., & Dias, R. J. (2016). Citric acid crosslinked cyclodextrin/hydroxypropylmethylcellulose hydrogel films for hydrophobic drug delivery. *International Journal of Biological Macromolecules, 93*, 75–86. https://doi.org/10.1016/j.ijbiomac.2016.08.072.

Gibbs, D. M. R., Black, C. R. M., Dawson, J. I., & Oreffo, R. O. C. (2016). A review of hydrogel use in fracture healing and bone regeneration: Hydrogel use in fracture healing and bone regeneration. *Journal of Tissue Engineering and Regenerative Medicine, 10*(3), 187–198. https://doi.org/10.1002/term.1968.

Gor'kov, P. L., Chekmenev, E. Y., Li, C., Cotten, M., Buffy, J. J., Traaseth, N. J., et al. (2007). Using low-E resonators to reduce RF heating in biological samples for static solid-state NMR up to 900MHz. *Journal of Magnetic Resonance, 185*(1), 77–93. https://doi.org/10.1016/j.jmr.2006.11.008.

Grasdalen, H. (1983). High-field, 1H-n.m.r. spectroscopy of alginate: sequential structure and linkage conformations. *Carbohydrate Research, 118*, 255–260. https://doi.org/10.1016/0008-6215(83)88053-7.

Gun'ko, V., Savina, I., & Mikhalovsky, S. (2017). Properties of water bound in hydrogels. *Gels, 3*(4), 37. https://doi.org/10.3390/gels3040037.

Guvendiren, M., & Burdick, J. A. (2013). Engineering synthetic hydrogel microenvironments to instruct stem cells. *Current Opinion in Biotechnology, 24*(5), 841–846. https://doi.org/10.1016/j.copbio.2013.03.009.

Hamcerencu, M., Desbrieres, J., Popa, M., & Riess, G. (2009). Stimuli-sensitive xanthan derivatives/ *N* -isopropylacrylamide hydrogels: Influence of cross-linking agent on interpenetrating polymer network properties. *Biomacromolecules, 10*(7), 1911–1922. https://doi.org/10.1021/bm900318g.

Hamcerencu, M., Desbrieres, J., Popa, M., & Riess, G. (2012). Original stimuli-sensitive polysaccharide derivatives/N-isopropylacrylamide hydrogels. Role of polysaccharide backbone. *Carbohydrate Polymers, 89*(2), 438–447. https://doi.org/10.1016/j.carbpol.2012.03.026.

Hamedi, H., Moradi, S., Hudson, S. M., & Tonelli, A. E. (2018). Chitosan based hydrogels and their applications for drug delivery in wound dressings: A review. *Carbohydrate Polymers, 199*, 445–460. https://doi.org/10.1016/j.carbpol.2018.06.114.

Han, Y., Ahn, J., Concel, J., Byeon, I.-J. L., Gronenborn, A. M., Yang, J., et al. (2010). Solid-state NMR studies of HIV-1 capsid protein assemblies. *Journal of the American Chemical Society, 132*(6), 1976–1987. https://doi.org/10.1021/ja908687k.

He, M., Wang, Z., Cao, Y., Zhao, Y., Duan, B., Chen, Y., et al. (2014). Construction of chitin/PVA composite hydrogels with jellyfish gel-like structure and their biocompatibility. *Biomacromolecules, 15*(9), 3358–3365. https://doi.org/10.1021/bm500827q.

Hecht, H., & Srebnik, S. (2016). Structural characterization of sodium alginate and calcium alginate. *Biomacromolecules, 17*(6), 2160–2167. https://doi.org/10.1021/acs.biomac.6b00378.

Hoffman, A. S. (2012). Hydrogels for biomedical applications. *Advanced Drug Delivery Reviews, 64*, 18–23. https://doi.org/10.1016/j.addr.2012.09.010.

Hou, G., Deng, F., Ding, S., Fu, R., Yang, J., & Ye, C. (2006). Quantitative cross-polarization NMR spectroscopy in uniformly ^{13}C-labeled solids. *Chemical Physics Letters, 421*(4–6), 356–360. https://doi.org/10.1016/j.cplett.2006.01.105.

Isogai, A., Usuda, M., Kato, T., Uryu, T., & Atalla, R. H. (1989). Solid-state CP/MAS carbon-13 NMR study of cellulose polymorphs. *Macromolecules, 22*(7), 3168–3172. https://doi.org/10.1021/ma00197a045.

Johnson, R. L., & Schmidt-Rohr, K. (2014). Quantitative solid-state ^{13}C NMR with signal enhancement by multiple cross polarization. *Journal of Magnetic Resonance, 239*, 44–49. https://doi.org/10.1016/j.jmr.2013.11.009.

Kaplan, M., Cukkemane, A., van Zundert, G. C. P., Narasimhan, S., Daniëls, M., Mance, D., et al. (2015). Probing a cell-embedded megadalton protein complex by DNP-supported solid-state NMR. *Nature Methods, 12*(7), 649–652. https://doi.org/10.1038/nmeth.3406.

Koers, E. J., van der Cruijsen, E. A. W., Rosay, M., Weingarth, M., Prokofyev, A., Sauvée, C., et al. (2014). NMR-based structural biology enhanced by dynamic nuclear polarization at high magnetic field. *Journal of Biomolecular NMR, 60*(2–3), 157–168. https://doi.org/10.1007/s10858-014-9865-8.

Kono, H. (2014). Characterization and properties of carboxymethyl cellulose hydrogels crosslinked by polyethylene glycol. *Carbohydrate Polymers, 106*, 84–93. https://doi.org/10.1016/j.carbpol.2014.02.020.

Kono, H., & Teshirogi, T. (2015). Cyclodextrin-grafted chitosan hydrogels for controlled drug delivery. *International Journal of Biological Macromolecules, 72*, 299–308. https://doi.org/10.1016/j.ijbiomac.2014.08.030.

Kono, H., Onishi, K., & Nakamura, T. (2013). Characterization and bisphenol A adsorption capacity of β-cyclodextrin–carboxymethylcellulose-based hydrogels. *Carbohydrate Polymers, 98*(1), 784–792. https://doi.org/10.1016/j.carbpol.2013.06.065.

Kono, H., Otaka, F., & Ozaki, M. (2014). Preparation and characterization of guar gum hydrogels as carrier materials for controlled protein drug delivery. *Carbohydrate Polymers, 111*, 830–840. https://doi.org/10.1016/j.carbpol.2014.05.050.

Kono, H., Yunoki, S., Shikano, T., Fujiwara, M., Erata, T., & Takai, M. (2002). CP/MAS ^{13}C NMR study of cellulose and cellulose derivatives. 1. Complete assignment of the CP/MAS ^{13}C NMR Spectrum of the native cellulose. *Journal of the American Chemical Society, 124*(25), 7506–7511. https://doi.org/10.1021/ja010704o.

Kopeček, J., & Yang, J. (2012). Smart self-assembled hybrid hydrogel biomaterials. *Angewandte Chemie International Edition, 51*(30), 7396–7417. https://doi.org/10.1002/anie.201201040.

Langer, B., Schnell, I., Spiess, H. W., & Grimmer, A.-R. (1999). Temperature calibration under ultrafast MAS conditions. *Journal of Magnetic Resonance, 138*(1), 182–186. https://doi.org/10.1006/jmre.1999.1717.

Lee, K. Y., & Mooney, D. J. (2012). Alginate: Properties and biomedical applications. *Progress in Polymer Science, 37*(1), 106–126. https://doi.org/10.1016/j.progpolymsci.2011.06.003.

Lenzi, F., Sannino, A., Borriello, A., Porro, F., Capitani, D., & Mensitieri, G. (2003). Probing the degree of crosslinking of a cellulose based superabsorbing hydrogel through traditional and NMR techniques. *Polymer, 44*(5), 1577–1588. https://doi.org/10.1016/S0032-3861(02)00939-4.

Li, B., Xu, L., Wu, Q., Chen, T., Sun, P., Jin, Q., et al. (2007). Various types of hydrogen bonds, their temperature dependence and water − polymer interaction in hydrated poly(acrylic acid) as revealed by ^{1}H solid-state NMR spectroscopy. *Macromolecules, 40*(16), 5776–5786. https://doi.org/10.1021/ma070485c.

Li, M., Mandal, A., Tyurin, V. A., DeLucia, M., Ahn, J., Kagan, V. E., et al. (2019). Surface-binding to cardiolipin nanodomains triggers cytochrome C pro-apoptotic peroxidase activity via localized dynamics. *Structure, 27*(5), https://doi.org/10.1016/j.str.2019.02.007 806-815.e4.

Lowe, I. J. (1959). Free induction decays of rotating solids. *Physical Review Letters, 2*(7), 285–287. https://doi.org/10.1103/PhysRevLett.2.285.

Mance, D., Sinnige, T., Kaplan, M., Narasimhan, S., Daniëls, M., Houben, K., et al. (2015). An efficient labelling approach to harness backbone and side-chain protons in ^{1}H-detected solid-state NMR spectroscopy. *Angewandte Chemie International Edition, 54*(52), 15799–15803. https://doi.org/10.1002/anie.201509170.

Mance, D., van der Zwan, J., Velthoen, M. E. Z., Meirer, F., Weckhuysen, B. M., Baldus, M., et al. (2017). A DNP-supported solid-state NMR study of carbon species in fluid catalytic cracking catalysts. *Chemical Communications, 53*(28), 3933–3936. https://doi.org/10.1039/C7CC00849J.

Mandal, A., Boatz, J. C., Wheeler, T. B., & van der Wel, P. C. A. (2017). On the use of ultracentrifugal devices for routine sample preparation in biomolecular magic-angle-spinning NMR. *Journal of Biomolecular NMR, 67*(3), 165–178. https://doi.org/10.1007/s10858-017-0089-6.

Mandal, A., Hoop, C. L., DeLucia, M., Kodali, R., Kagan, V. E., Ahn, J., et al. (2015). Structural changes and proapoptotic peroxidase activity of cardiolipin-bound mitochondrial cytochrome c. *Biophysical Journal, 109*(9), 1873–1884. https://doi.org/10.1016/j.bpj.2015.09.016.

Marassi, F. M., & Crowell, K. J. (2003). Hydration-optimized oriented phospholipid bilayer samples for solid-state NMR structural studies of membrane proteins. *Journal of Magnetic Resonance, 161*(1), 64–69.

Martin, R. W., & Zilm, K. W. (2003). Preparation of protein nanocrystals and their characterization by solid state NMR. *Journal of Magnetic Resonance, 165*(1), 162–174. https://doi.org/10.1016/S1090-7807(03)00253-2.

Matlahov, I., & van der Wel, P. C. A. (2018). Hidden motions and motion-induced invisibility: Dynamics-based spectral editing in solid-state NMR. *Methods, 148*, 123–135. https://doi.org/10.1016/j.ymeth.2018.04.015.

Medeiros-Silva, J., Jekhmane, S., Paioni, A. L., Gawarecka, K., Baldus, M., Swiezewska, E., et al. (2018). High-resolution NMR studies of antibiotics in cellular membranes. *Nature Communications, 9*(1), https://doi.org/10.1038/s41467-018-06314-x.

Mollica, G., Ziarelli, F., Lack, S., Brunel, F., & Viel, S. (2012). Characterization of insoluble calcium alginates by solid-state NMR. *Carbohydrate Polymers, 87*(1), 383–391. https://doi.org/10.1016/j.carbpol.2011.07.066.

Naahidi, S., Jafari, M., Logan, M., Wang, Y., Yuan, Y., Bae, H., et al. (2017). Biocompatibility of hydrogel-based scaffolds for tissue engineering applications. *Biotechnology Advances, 35*(5), 530–544. https://doi.org/10.1016/j.biotechadv.2017.

05.006.
Narayanaswamy, R., & Torchilin, V. P. (2019). Hydrogels and their applications in targeted drug delivery. *Molecules, 24*(3), 603. https://doi.org/10.3390/molecules24030603.
Nardecchia, S., Gutiérrez, M. C., Serrano, M. C., Dentini, M., Barbetta, A., Ferrer, M. L., et al. (2012). In situ precipitation of amorphous calcium phosphate and ciprofloxacin crystals during the formation of chitosan hydrogels and its application for drug delivery purposes. *Langmuir, 28*(45), 15937–15946. https://doi.org/10.1021/la3033435.
Nonappa, N., & Kolehmainen, E. (2016). Solid state NMR studies of gels derived from low molecular mass gelators. *Soft Matter, 12*(28), 6015–6026. https://doi.org/10.1039/C6SM00969G.
Polenova, T., Gupta, R., & Goldbourt, A. (2015). Magic angle spinning NMR spectroscopy: A versatile technique for structural and dynamic analysis of solid-phase systems. *Analytical Chemistry, 87*(11), 5458–5469. https://doi.org/10.1021/ac504288u.
Radloff, D., Boeffel, C., & Spiess, H. W. (1996). Cellulose and cellulose/poly(vinyl alcohol) blends. 2. Water organization revealed by solid-state NMR spectroscopy. *Macromolecules, 29*(5), 1528–1534. https://doi.org/10.1021/ma950405h.
Rad-Malekshahi, M., Visscher, K. M., Rodrigues, J. P. G. L. M., de Vries, R., Hennink, W. E., Baldus, M., et al. (2015). The supramolecular organization of a peptide-based nanocarrier at high molecular detail. *Journal of the American Chemical Society, 137*(24), 7775–7784. https://doi.org/10.1021/jacs.5b02919.
Ramalhete, S. M., Nartowski, K. P., Sarathchandra, N., Foster, J. S., Round, A. N., Angulo, J., et al. (2017). Supramolecular amino acid based hydrogels: Probing the contribution of additive molecules using NMR spectroscopy. *Chemistry - A European Journal, 23*(33), 8014–8024. https://doi.org/10.1002/chem.201700793.
Remminghorst, U., & Rehm, B. H. A. (2006). Bacterial alginates: From biosynthesis to applications. *Biotechnology Letters, 28*(21), 1701–1712. https://doi.org/10.1007/s10529-006-9156-x.
Renault, M., Shintu, L., Piotto, M., & Caldarelli, S. (2013). Slow-spinning low-sideband HR-MAS NMR spectroscopy: Delicate analysis of biological samples. *Scientific Reports, 3*(1), 3349. https://doi.org/10.1038/srep03349.
Salomonsen, T., Jensen, H. M., Stenbæk, D., & Engelsen, S. B. (2008). Chemometric prediction of alginate monomer composition: A comparative spectroscopic study using IR, Raman, NIR and NMR. *Carbohydrate Polymers, 72*(4), 730–739. https://doi.org/10.1016/j.carbpol.2007.10.022.
Salomonsen, T., Jensen, H. M., Larsen, F. H., Steuernagel, S., & Engelsen, S. B. (2009a). Alginate monomer composition studied by solution- and solid-state NMR – A comparative chemometric study. *Food Hydrocolloids, 23*(6), 1579–1586. https://doi.org/10.1016/j.foodhyd.2008.11.009.
Salomonsen, T., Jensen, H. M., Larsen, F. H., Steuernagel, S., & Engelsen, S. B. (2009b). Direct quantification of M/G ratio from ^{13}C CP-MAS NMR spectra of alginate powders by multivariate curve resolution. *Carbohydrate Research, 344*(15), 2014–2022. https://doi.org/10.1016/j.carres.2009.06.025.
Samal, S. K., Dash, M., Dubruel, P., & Van Vlierberghe, S. (2014). 8 - Smart polymer hydrogels: Properties, synthesis and applications. In M. R. Aguilar, & J. San Román (Eds.). *Smart polymers and their applications* (pp. 237–270). Woodhead Publishing. https://doi.org/10.1533/9780857097026.1.237.
Sarkar, R., Mainz, A., Busi, B., Barbet-Massin, E., Kranz, M., Hofmann, T., et al. (2016). Immobilization of soluble protein complexes in MAS solid-state NMR: Sedimentation versus viscosity. *Solid State Nuclear Magnetic Resonance, 76–77*, 7–14. https://doi.org/10.1016/j.ssnmr.2016.03.005.
Schaefer, J., & Stejskal, E. O. (1976). Carbon-13 nuclear magnetic resonance of polymers spinning at the magic angle. *Journal of the American Chemical Society, 98*(4), 1031–1032. https://doi.org/10.1021/ja00420a036.
Schmidt, J. E., Peng, L., Paioni, A. L., Ehren, H. L., Guo, W., Mazumder, B., et al. (2018). Isolating clusters of light elements in molecular sieves with atom probe tomography. *Journal of the American Chemical Society, 140*(29), 9154–9158. https://doi.org/10.1021/jacs.8b04494.
Shapiro, Y. E. (2011). Structure and dynamics of hydrogels and organogels: An NMR spectroscopy approach. *Progress in Polymer Science, 36*(9), 1184–1253. https://doi.org/10.1016/j.progpolymsci.2011.04.002.
Shariatinia, Z. (2018). Carboxymethyl chitosan: Properties and biomedical applications. *International Journal of Biological Macromolecules, 120*, 1406–1419. https://doi.org/10.1016/j.ijbiomac.2018.09.131.
Silva, T. H., Alves, A., Ferreira, B. M., Oliveira, J. M., Reys, L. L., Ferreira, R. J. F., et al. (2012). Materials of marine origin: A review on polymers and ceramics of biomedical interest. *International Materials Reviews, 57*(5), 276–306. https://doi.org/10.1179/1743280412Y.0000000002.
Singh, B., & Singh, B. (2018). Modification of sterculia gum polysaccharide via network formation by radiation induced crosslinking polymerization for biomedical applications. *International Journal of Biological Macromolecules, 116*, 91–99. https://doi.org/10.1016/j.ijbiomac.2018.05.032.
Singh, B., Dhiman, A., Rajneesh, & Kumar, A. (2016). Slow release of ciprofloxacin from β- cyclodextrin containing drug delivery system through network formation and supramolecular interactions. *International Journal of Biological Macromolecules, 92*, 390–400. https://doi.org/10.1016/j.ijbiomac.2016.07.060.
Singh, B., Varshney, L., Francis, S., & Rajneesh (2016). Designing tragacanth gum based sterile hydrogel by radiation method for use in drug delivery and wound dressing applications. *International Journal of Biological Macromolecules, 88*, 586–602. https://doi.org/10.1016/j.ijbiomac.2016.03.051.
Smidsrød, O., & Skjåk-Braek, G. (1990). Alginate as immobilization matrix for cells. *Trends in Biotechnology, 8*, 71–78. https://doi.org/10.1016/0167-7799(90)90139-O.
Smith, A. N., Märker, K., Piretra, T., Boatz, J. C., Matlahov, I., Kodali, R., et al. (2018). Structural fingerprinting of protein aggregates by dynamic nuclear polarization-enhanced solid-state NMR at natural isotopic abundance. *Journal of the American Chemical Society, 140*(44), 14576–14580. https://doi.org/10.1021/jacs.8b09002.
Sparrman, T., Svenningsson, L., Sahlin-Sjövold, K., Nordstierna, L., Westman, G., & Bernin, D. (2019). A revised solid-state NMR method to assess the crystallinity of cellulose. *Cellulose, 26*(17), 8993–9003. https://doi.org/10.1007/s10570-019-02718-0.
Sperger, D. M., Fu, S., Block, L. H., & Munson, E. J. (2011). Analysis of composition, molecular weight, and water content variations in sodium alginate using solid-state NMR spectroscopy. *Journal of Pharmaceutical Sciences, 100*(8), 3441–3452. https://doi.org/10.1002/jps.22559.
Stringer, J. A., Bronnimann, C. E., Mullen, C. G., Zhou, D. H., Stellfox, S. A., Li, Y., et al. (2005). Reduction of RF-induced sample heating with a scroll coil resonator structure for solid-state NMR probes. *Journal of Magnetic Resonance, 173*(1), 40–48. https://doi.org/10.1016/j.jmr.2004.11.015.
Takeda, K., Noda, Y., Takegoshi, K., Lafon, O., Trébosc, J., & Amoureux, J.-P. (2012). Quantitative cross-polarization at magic-angle spinning frequency of about 20kHz. *Journal of Magnetic Resonance, 214*, 340–345. https://doi.org/10.1016/j.jmr.2011.11.014.
Tamesue, S., Takashima, Y., Yamaguchi, H., Shinkai, S., & Harada, A. (2010). Photoswitchable supramolecular hydrogels formed by cyclodextrins and azobenzene polymers. *Angewandte Chemie International Edition, 49*(41), 7461–7464. https://doi.org/10.1002/anie.201003567.
Thu, B., Bruheim, P., Espevik, T., Smidsrød, O., Soon-Shiong, P., & Skjåk-Bræk, G. (1996). Alginate polycation microcapsules: II. Some functional properties. *Biomaterials, 17*(11), 1069–1079. https://doi.org/10.1016/0142-9612(96)85907-2.
Tønnesen, H. H., & Karlsen, J. (2002). Alginate in drug delivery systems. *Drug Development and Industrial Pharmacy, 28*(6), 621–630. https://doi.org/10.1081/DDC-120003853.
Urbanova, M., Pavelkova, M., Czernek, J., Kubova, K., Vyslouzil, J., Pechova, A., et al. (2019). Interaction pathways and structure–chemical transformations of alginate gels in physiological environments. *Biomacromolecules, 20*(11), 4158–4170. https://doi.org/10.1021/acs.biomac.9b01052.
Urtuvia, V., Maturana, N., Acevedo, F., Peña, C., & Díaz-Barrera, A. (2017). Bacterial alginate production: An overview of its biosynthesis and potential industrial production. *World Journal of Microbiology & Biotechnology, 33*(11), https://doi.org/10.1007/s11274-017-2363-x.
Usov, A. I. (1999). Alginic acids and alginates: Analytical methods used for their estimation and characterisation of composition and primary structure. *Russian Chemical Reviews, 68*(11), 957–966. https://doi.org/10.1070/RC1999v068n11ABEH000532.
van der Wel, P. C. A. (2017). Insights into protein misfolding and aggregation enabled by solid-state NMR spectroscopy. *Solid State Nuclear Magnetic Resonance, 88*, 1–14. https://doi.org/10.1016/j.ssnmr.2017.10.001.
van der Wel, P. C. A. (2018). New applications of solid-state NMR in structural biology. *Emerging Topics in Life Sciences, 2*(1), 57–67. https://doi.org/10.1042/ETLS20170088.
van Zandvoort, I., Koers, E. J., Weingarth, M., Bruijnincx, P. C. A., Baldus, M., & Weckhuysen, B. M. (2015). Structural characterization of ^{13}C-enriched humins and alkali-treated ^{13}C humins by 2D solid-state NMR. *Green Chemistry, 17*(8), 4383–4392. https://doi.org/10.1039/C5GC00327J.
Vermonden, T., Censi, R., & Hennink, W. E. (2012). Hydrogels for protein delivery. *Chemical Reviews, 112*(5), 2853–2888. https://doi.org/10.1021/cr200157d.
Weingarth, M., & Baldus, M. (2013). Solid-state NMR-based approaches for supramolecular structure elucidation. *Accounts of Chemical Research, 46*(9), 2037–2046. https://doi.org/10.1021/ar300316e.
Wang, F., Zhang, R., Chen, T., & Sun, P. (2016). ^{2}H solid-state NMR analysis of the dynamics and organization of water in hydrated chitosan. *Polymers, 8*(4), 149. https://doi.org/10.3390/polym8040149.
Weingarth, M., Ader, C., Melquiond, A. S. J., Nand, D., Pongs, O., Becker, S., et al. (2012). Supramolecular structure of membrane-associated polypeptides by combining solid-state NMR and molecular dynamics simulations. *Biophysical Journal, 103*(1), 29–37. https://doi.org/10.1016/j.bpj.2012.05.016.
Yahia, L. (2015). History and applications of hydrogels. *Journal of Biomedical Sciences, 4*(2), https://doi.org/10.4172/2254-609X.100013.
Yang, H.-C., Wang, W.-H., Huang, K.-S., & Hon, M.-H. (2010). Preparation and application of nanochitosan to finishing treatment with anti-microbial and anti-shrinking properties. *Carbohydrate Polymers, 79*(1), 176–179. https://doi.org/10.1016/j.carbpol.2009.07.045.
Yang, K., & Zeng, M. (2013). Multiresponsive hydrogel based on polyacrylamide functionalized with thymine derivatives. *New Journal of Chemistry, 37*(4), 920. https://doi.org/10.1039/c3nj41013g.
Yuk, H., Varela, C. E., Nabzdyk, C. S., Mao, X., Padera, R. F., Roche, E. T., et al. (2019). Dry double-sided tape for adhesion of wet tissues and devices. *Nature, 575*(7781), 169–174. https://doi.org/10.1038/s41586-019-1710-5.